Designing of Masks for Quantum Dot Single Electron Transistor Fabrication using E-beam Nanolithography

U. Hashim, Sutikno and Z.A.Z. Jamal

School of Microelectronic Engineering,
University of Malaysia Perlis (UniMAP), Kawasan Bank Pembangunan,
Kuala Perlis, 02000, Malaysia, uda@kukum.edu.my

ABSTRACT

Quantum dot single electron transistor (QD SET) is able to be fabricated through a joint technique of e-beam lithography (EBL), pattern dependent oxidation (PADOX) and high density plasma etching. In this research, we have fabricated amount of masks for preliminary works in preparation of single electron transistor design. In detail, one of them is mask for doped area separator and others are for formation of source-QD-drain, poly-Si gate, point contact and metal pad. They all are designed using GDSII Editor software offline and then exposed using SEM based EBL. In this paper, we demonstrate all of patterned masks and their nanostructures of SEM and atomic force microscopy (AFM). Shape and dimension biases of schematics and SEM images are found where it is accused by proximity effect, design dimension and inaccurately plane of focus.

Keywords: SEM based EBL, mask design, proximity effect, resist dot, nano patterning

1 INTRODUCTION

There are three common types of SETs such as nano wire, carbon nano tube (CNT) and QD SET that it basically consists of major structure of a conventional gate capacitor and two tunneling capacitors forming source and drain [1,18]. Two different methodologies have been proposed for fabrication of silicon quantum dot in previously published papers: (i) a bottom up and (ii) top-down approach. EBL is the most commonly used technique in this field, and many researchers have been investigating how to use it to make nanopatterns, such as Fulton and Dolan made SETs using an offset mask technique [19]. By using EBL to define the QD instead of stress dependent oxidation rate, the size and shape of dot can be better controlled [7].EBL is currently the production technique of masks used for other kinds of lithography. Its resolution will mean that it is always the choice for direct-write one-off production [14]. The amount of masks used in SET fabrication process depends strongly on each route of process where as they decrease, SET fabrication process will be simpler. Several attempts have therefore been made to develop a technique where different layers or function parts of the SET device are prepared in separate lithography steps [22]. In general, researchers have used some masks in their SETs fabrication such as masks for formation of point contact pad [17,18], poly-Si gate [10,2], metal pad and for ion implantation [18,16], plasma oxide maso of Si etching [15,11] or defining Si structure [10]. Even additional masks are frequently applicable for SET fabrication such as aluminium sacrificial [5,21] or suspended mask [12]. Constrictions as tunnel barriers enable to be fabricated using etch mask that defined by EBL [3,23]. In this paper, we report techniques how to design, optimize and fabricate masks for SET fabrication.

2 EXPERIMENTAL PROCEDURES

Square substrates of 15 mm x 15 mm in size prepared of silicon wafer in specifications of <100> crystal orientation, P/B type/dopant, diameter of about 525 nm and resistivity of 1 to 10 ohm.cm, are as the starting materials. Wafer silicon cut in parallel to the shortest wafer diameter is to prevent the unbroken wafer. Such square substrates with straight sides of 3 minimum are to easily place in adjusting stage position when focusing SEM image, therewith we will able to observe design patterns on the developed resist.

Wafer is first cleaned to remove either organic or inorganic contaminants using standard cleaning 1 with procedures like the following: dip in RCA-1 solution at temperature 75ºC for 10 minutes, rinse in de-ionized (DI) water, dip in buffer oxide etch (BOE) for 10-15 minutes, rinse in DI-water, dip in RCA-2 solution at temperature 80ºC for 10-15 minutes, rinse in DI-water and then dried on the spinner. In addition, RCA-1 and RCA-2 solutions were heated up to 75ºC and 80ºC using corning hotplate.

The dried substrates were heated up to 200ºC for 30 minutes using conduction hotplate JB-TEK Honeywall and thereafter cooled down to room temperature. So It is currently ready to be exposed using EBL. Meanwhile, mask 4 is specifically spin coated with 495 PMMA positive resist on the ramp up of 500 rpm for 6 seconds, spin speed of 400 rpm for 30 seconds and ramp down of 0 rpm for 5 seconds.

Such masks were designed using offline GDSII Editor software by considering proximity effects, optimum resolution of resist and e-beam equipment. In this research, we have fabricated five masks consist of doped area separator mask and masks for source-QD-drain, poly-Si

gate, point contact and Al metal pad formation. The reason for the size difference is considered to be effects of the resolution of the lithography in which the optimum resolution of ma-N 2403 negative resist is 50 nm and minimum area step size of version 4.0 Raith software EBL is 40 nm. However, single QD is designed in the range of that equipment resolution and in fact biases of resist pattern width of SEM micrograph images are frequently found 80 nm wider than that of GDSII design. Mask 4 was specifically spun of 495 PMMA (polymetylmetacrylate) A4 resist 4% in anisole and while others were spun of ma-N 2403 negative resist.

To expose pattern design on the resist surface, EBL system is first set up as follows: 20 kV accelerating voltage, 45 spot size, 200 micron field size, 450X microscope magnification and e-beam dose ranges from 180 $\mu As/cm^2$ to 235 $\mu As/cm^2$. After e-beam exposure, SEM vacuum chamber is vented to take out sample. Subsequently, samples were developed in a methyl-isobutyl-ketone (MIBK, PMMA solvent) mixed with three parts of isopropyl alcohol (IPA, non solvent) to obtain higher contrast [13] for 30 seconds and then dipped in IPA for 15 seconds to 30 seconds. The developed nanostructures were then characterized by using SEM (JEOL SEM 6460LA) and atomic force microscopy (AFM SPI Probe Station 3800N, SPA400 Sound Proof Housing).

3 RESULTS AND DISCUSSIONS

Figure 1(a) is a schematic drawing of mask 1 that used to insulate un-doped area of doped area during doping process done. If dimension of mask 1 as shown in Fig. 1(a) we compare with dimension of SEM image as shown in Fig. 1(b), we could observe that in Fig. 1(b) appears the lower part width of resist mask 1 is about 176 nm and the upper part width of resist mask 1 is 462 nm. The total length of mask 1 is 798 nm while the dark part length is 607 nm. The resist mask 1 with 23.36 nm peak height is measurable through profile line analysis of AFM image as shown in Fig. 1(c) where it seems uniformly flat. SEM image shows blunt mask edges and imaged dimensions biased of initial dimensions. Many researchers have used implantation mask in their doping process [9,16]. Meantime Kobayashi et al. (2006) have used this mask as suspended mask.

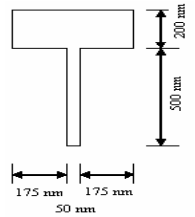

(a)

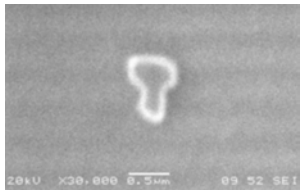

(b)

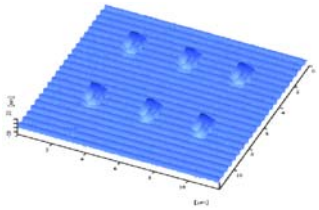

(c)

Figure 1. (a) Schematic drawing of mask 1, (b) SEM image of mask 1 and (c) AFM image of mask 1.

Figure 2(a) is a schematic drawing of mask 2 for source-QD-drain formation. Subsequently figure 2(b) shows a resist dot between masks of source and drain which have minimum source dimension of 767 nm x 591 nm and drain dimension of 740 nm x 552 nm. Meanwhile, especially dot diameter like Fig. 2(b) is 297 nm and the dot diameters of AFM images range from 134 nm to 161 nm. On the other hand, in three dimensions, these resist nano dots seem like cones as shown in Fig. 2(c). We have fabricated many samples and found that the peak height of cone nano dots is in the range of about 10 nm to 200 nm. Both of area spaces between source-dot and dot-drain resist mask function as nano constrictions (tunnel barriers). The design of nano constrictions were varied to observe the optimum dimension.

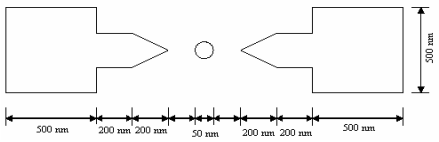

(a)

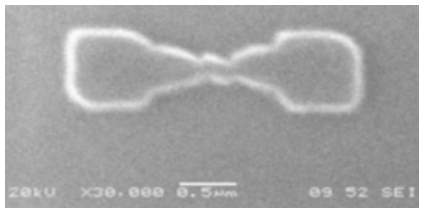

(b)

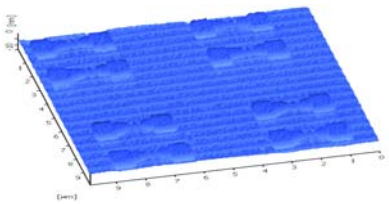

(c)

Figure 2. (a) Schematic drawing of mask 2, (b) SEM image of mask 2 and (c) AFM image of mask 2.

Figure 3(a) is a schematic drawing of mask 3 that used to form poly-Si top gate. Basically design of mask 3 is the same as mask 1 where this equity is devised for accurately alignment. Image in Fig. 3(b) seems narrower than that of Fig. 1(b), in addition, mask 1 is resulted at condition under development and inversely mask 3 is resulted at over one condition. In this research, sufficiently small area step size and e-beam dose will result deflected lines of SEM image.

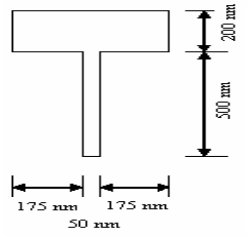

(a)

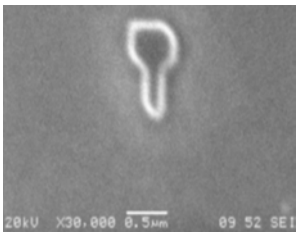

(b)

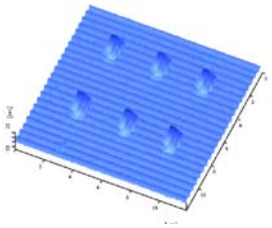

(c)

Figure 3. (a) Schematic drawing of mask 3, (b) SEM image of mask 3 and (c) AFM image of mask 3.

Figure 4(a) is schematic of mask 4 for point contact formation and Fig. 4(c) is image of such mask that captured under AFM and then to complete these characterizations, it is also viewed under SEM. In fact SEM image of mask 4 shows lighter pattern than background and on the other hand, SEM images of others masks inversely show darker pattern. In addition, point contact patterns spin coated of positive resist seem like holes and inversely point contact patterns spin coated of negative resist like peaks. The lighter color of pattern lines of negative resist is a trend side profile. The width of negative resist pattern lines can be optimized by focusing SEM. Fig. 4(b) shows point contact mask of 294 nm width and the hole depth of mask 4 is 7.41 nm. Schematic of mask 4 are squares but in SEM image seems circles. Therewith we found shape bias of mask schematics and SEM images of mask where according to Hudek & Beyer (2006), this is accused by proximity effects. Therefore, existing correction techniques rely on (i) shot-by-shot modulation of the exposure dose, (ii) modification of pattern geometry (shape bias), or on (iii) combining of both methods [8].

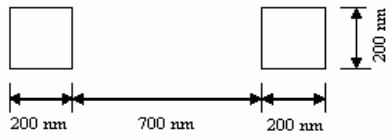

(a)

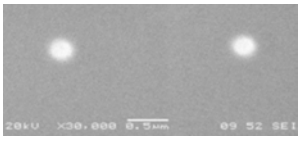

(b)

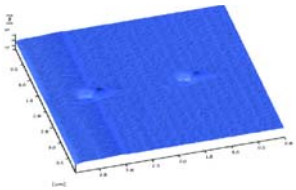

(c)

Figure 4. (a) Schematic drawing of mask 4, (b) SEM image of mask 4 and (c) AFM image of mask 4.

Metal pad mask of this SET design is schematically drawn as shown in Fig. 5(a). Figure 5(c) shows AFM image of mask for metal pad formation, where for fabrication of this mask will be used aluminium as an alternative metal pad material. In figure 5(b), the dimensions of this mask are as the followings: side width of 693 nm, center width of 568 nm and the length of 1.206 nm. In three dimensions, Fig. 5(c) shows the peak height of resist mask of 14.41 nm. Equipment-related parameters are also critical in nano-patterning, when a variable-shape pattern generator is used for resist exposure. All of masks show that the line edges are not sharp. In this context, the line edges were defined by the shape of the circle beam shots. Therefore, to enhance edge line sharpness, it is recommended to use a rectangular beam shots. The line-edge roughness is defined mainly by the shape of the rectangular beam shots, and the stitching errors at the joint-point of two shots. These two problems are influenced by the quality of the rectangular apertures and the alignment of the e-beam formation system [14].

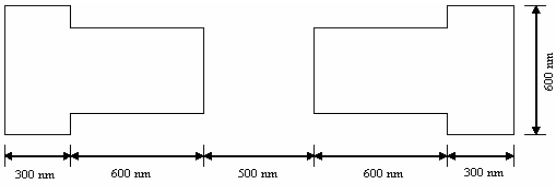

(a)

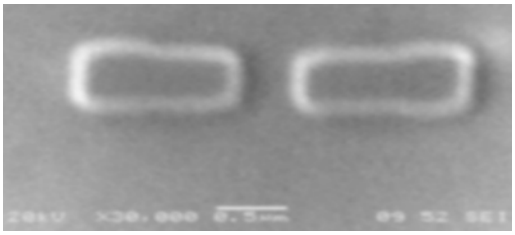
(b)

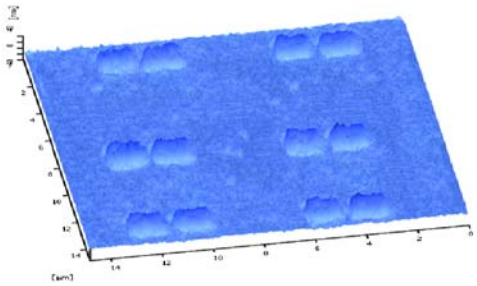
(c)

Figure 5. (a) Schematic drawing of mask 5, (b) SEM image of mask 5 and (c) AFM image of mask 5.

4 CONCLUSIONS

In conclusion, direct write EBL is a useful technique for fabrication of QD SET masks with small critical dimension. The EBL resolution is limited not by e-beam diameter, but by a combination of proximity effects, resist chemistry and e-beam alignment. In this work, direct write EBL process was optimized to fabricate different types of masks. Recently fabrication of cone nano dots that ranges from 134 nm to 161 nm has been demonstrated for negative resist and fabrication of point contacts of 294 nm has also been demonstrated for positive resist. The other masks have been fabricated of negative resist in the range of above 153 nm.

5 ACKNOWLEDMENT

The financial support of Graduate Assistance (GA) Program of KUKUM (the former name) or UniMAP (the current name) is kindly acknowledged. Consumables, gases and chemicals used in this research are supported by IRPA Project, Malaysian Ministry of Science, Technology and Innovation (MOSTI) under grant No. IRPA 09-02-15-0000-SR0013/06-060.

REFERENCES

[1] S. Altmeyer, B. Spangenberg, F. Kühnel, Microelectron. Eng., 30, 399-402, 1996.
[2] T. Berrer, D. Pachinger, G. Pillwein, M. Mühlberger, H. Lightenberger, G. Brunthaler, F. Schäffler, Physica E34, 572-578, 2006.
[3] M. Dilger, R.J. Haugh, K.V. Klitzing, Semicond. Sci. Technol., 11, 1493-1497, 1996.
[4] Z.A.K. Durrani, Physica, E17, 572-578, 2003.
[5] E.G. Emiroglu, D.G. Hasko, D.A. Williams, Microelectron. Eng., 73-74, 701-706, 2004.
[6] Y. Furuta, H. Mizuta, T. Kamiya, Y.T. Tan, K. Nakazato, Z.A.K. Durrani, K. Taniguchi, ESSDRC, 399-402, 2002.
[7] U. Hashim, Sutikno and Z.A.Z. Jamal, Proc. of ICMNS'06 Institut Teknologi Bandung, 2006.
[8] P. Hudek and D. Beyer, Microelectron. Eng., 780-783, 2006.
[9] F.E. Hudson, A.J. Ferguson, D.N. Jamieson, A.S. Dzurak and R.G. Clark, Microelectron. Eng., 83, 1809-1813, 2006.
[10] S.F. Hu, G.J. Wang, Y.P. Fang, Z.Y. Pan, Y.C. Chou, Chinese Journal of Phys., 42(5), 636-642, 2004.
[11] Y. Ito, H. Tsuyoshi, N. Anri, Yokoyama, Appl. Phys. Lett., 80(24), 4617-4619, 2002.
[12] S. Kobayashi, M. Imaeda, S, Matsumoto, Materials Sci. & Eng., c26, 889-892, 2006.
[13] A. Kowalik, Z. Jaroszewcz, A. Kolodzejcyk, Microelectron. Eng., 77, 347-357, 2005.
[14] I. Kostic, R. Andok, V. Barak, I. Caplovic, A. Konecnikova, L. Mattay, P. Hrkut, A. Ritomsky, J. Matter. Sci., 14, 645-648, 2003.
[15] K. Kurihara, H. Namatsu, M. Nagase, T. Makino, Microelectron. Eng., 35, 261-264, 1997.
[16] M. Mitic, S.E. Andresen, C. Yang, T. Hopf, V. Chan, E. Gauja, F.E. Hudson, T.M. Buehler, A.J. Ferguson, C.I. Pakes, S.M. Hearne, G. Tamanyan, D.J. Reilly, A.R. Hamilton, D.N. Jamielson, A.S. Dzurak, R.G. Clark, Microelectron. Eng., 78-79, 279-286, 2005.
[17] A. Notargiacomo, L.D. Gaspare, G. Scappuci, G. Mariottini, E. Giovine, F. Evangelisti, Materials Sci. and Eng., C23, 671-673, 2003.
[18] L. Palun, S. Tedesco, M . Heitzman, F. Martin, D. Fraboulet, B. Dal'zotto, M.E. Nier, P. Mur, T. Charvolin, Microelectron. Eng., 53, 167-170, 2003.
[19] T.R. Stevenson, W.T. Hsieh, M.J. Li, K.W. Rhee, R.J. Schoelkopf, C.M. Stahle, J.D. Teufel, IEEE Trans. Appl. Supercond., 13(2), 1139-1142, 2003.
[20] Y. Takahashi, Y. Ono, A. Fujiwara, H. Inokawa, NTT Technical Review, 2(2), 21-27, 2004.
[21] M.G. Tanner, E.G. Emiroglu, D.G. Hasko, D.A. Williams, Microelectron. Eng., 53, 225-228, 2000.
[22] T. Weinmann, H. Scherer, P. Hinze, J. Niemeyer, Microelectron. Eng., 53, 225-228, 2000.
[23] L .Zhuang, L. Guo, S.Y. Chou, Appl. Phys. Lett., 72(10), 1205-1207, 1998.